The Ku70 DNA-repair protein is involved in centromere function in a grasshopper species

Josefa Cabrero · Mohammed Bakkali · Beatriz Navarro-Domínguez · Francisco J. Ruíz-Ruano · Rubén Martín-Blázquez · Mª Dolores López-León · Juan Pedro M. Camacho*

Departamento de Genética, Facultad de Ciencias, Universidad de Granada

* E-mail: jpmcamac@ugr.es

Short title: Centromere function for the Ku70 protein

Abstract The Ku70 protein is involved in numerous cell functions, the non-homologous end joining (NHEJ) DNA repair pathway being the best known. Here we report a novel function for this protein in the grasshopper *Eyprepocnemis plorans*. We observed the presence of large Ku70 *foci* on the centromeres of meiotic and mitotic chromosomes during the cell cycle stages showing the highest centromeric activity (i.e. metaphase and anaphase). The fact that colchicine treatment prevented centromeric location of Ku70, suggests a microtubule-dependent centromeric function for Ku70. Likewise, the absence of Ku70 at metaphase-anaphase centromeres from three males whose *Ku70* gene had been knocked down using RNAi, and the dramatic increase in the frequency of polyploid spermatids observed in these males, suggest that the centromeric presence of Ku70 is required for normal cytokinesis in this species. The centromeric function of Ku70 was not observed in 14 other grasshopper and locust species, nor in the mouse, thus suggesting that it is an autapomorphy in *E. plorans*.

Keywords: Autapomorphy; centromere; *Eyprepocnemis plorans*; gene knockdown; immunofluorescence; kinetochore; Ku70; Ku80; microtubules; Orthoptera; RNAi; spindle assembly checkpoint.

Abbreviations

+TIPs	Plus-ends of growing microtubules
APC	Adenomatous polyposis coli protein
DAPI	4',6-diamidino-2-phenylindole
dffi	days from the first injection
DNA-PKcs	DNA-dependent protein kinase catalytic subunit
DSB	Double stranded DNA breaks
EB1	End binding 1 protein
FIA	Feulgen Image Analysis
γH2AX	phosphorylated form of the H2AX histone
GAPDH	glyceraldehyde-3-phosphate dehydrogenase
HR	Homologous recombination
MT	microtubules
NHEJ	Non-homologous end joining
RNAi	Interference RNA
RP49	ribosomal protein 49
SAC	spindle assembly checkpoint

Introduction

Eukaryotic cells repair double stranded DNA breaks (DSB) via two pathways: homologous recombination (HR) and non-homologous end-joining (NHEJ), both playing a role in maintaining chromosomal DNA throughout the cell cycle (Takata et al. 1998). Among the several proteins involved in these pathways, Ku is a heterodimer of two polypeptides of about 69 and 83 kD, called Ku70 and Ku80 (or Ku86) respectively. It is a multifunctional protein involved directly or indirectly in many important cellular metabolic processes, such as DNA DSB repair through the NHEJ pathway, V(D)J recombination of immunoglobulins and T-cell receptor genes, immunoglobulin isotype switching, DNA replication, transcription regulation, heat-shock response, telomere maintenance, and cell-cycle regulation (Tuteja and Tuteja 2000). Such a variety of functions is derived from the ability of Ku to bind to DNA, RNA, and proteins. The DNA repair function of this protein is performed in conjunction with the DNA-dependent protein kinase catalytic subunit (DNA-PKcs), with which it forms the DNA-dependent protein kinase (Gell and Jackson 1999). It has been suggested that the monomer Ku70 (on which this work focuses) acts as a switch between the HR and NHEJ DSB repair pathways, so that downregulation of Ku70 in early meiosis (pre-leptotene-zygotene) may ensure that meiotic DSBs are processed by homologous recombination (Goedecke et al. 1999). Phylogenetic analysis of Ku70 orthologs in fungi, plants and animals has revealed that the Ku70 protein is highlyconserved among eukaryotes (Pöggeler and Kuck 2006).

Being components of the nuclear matrix, Ku proteins are predominantly nuclear, where they appear diffusely distributed throughout the nucleoplasm (Koike et al. 1999). However, in addition to its DNA-repair function in the nucleus, Ku70 has been located

in the cytoplasm, where it can inhibit Bax-mediated apoptosis (Sawada et al. 2003). It has also been found in the plasma membrane, where it can participate in heterologous and homologous cell adhesion (Koike 2002) as well as fibronectin binding (Monferran et al. 2004a), and can interact with metalloprotease 9 (MMP-9) (Monferran et al. 2004b). Furthermore, a binding site for Ku70/80 has been found in LINE-1 retrotransposons, suggesting that these proteins may also participate in transposition (Katz et al. 2005).

Ku moves rapidly throughout the nucleus, showing a transient high-flux association with nuclear substrates, including both DNA and the nuclear matrix —the latter associating only with the Ku70 monomer (Rodgers et al. 2002). As if the Ku functional picture wasn´t complex enough, several reports suggest that this protein may have additional functions that are independent of the DNA-dependent protein kinase holoenzyme (Gao et al. 1998; Gu et al. 2000). Evenmore, the Ku70 monomer was suggested to possibly have functions that are independent of Ku80 (Koike et al. 2001). Consistently, it has been reported that Ku70 and Ku80 monomers can show independent location in the nucleus (Bertinato et al. 2001). It has also been shown that Ku70, but not Ku80, interacts with heterochromatin protein 1α (HP1α) —a protein known to be associated with telomeres and heterochromatin (Song et al. 2001). Likewise, Ku70 seems to be involved in the internalization of the obligate intracellular bacterium *Rickettsia conorii* (Martinez et al. 2005). It has also been suggested that Ku80 has a Ku70-independent DNA DSB repair function, in addition to the one dependent on Ku70 (Koike and Koike 2005).

Throughout our several studies on supernumerary (B) chromosomes (a kind of parasitic chromosomes), we consistently came across several effects of these chromosomes in the grasshopper *Eyprepocnemis plorans*, e.g. decreasing egg fertility

(Zurita et al. 1998; Muñoz et al. 1998) or increasing the frequency of chiasmata (the cytological manifestation of meiotic recombination) in the host genome (Camacho et al. 1980; 2002). To determine the molecular causes of chiasma frequency changes, we analyzed whether the presence of B chromosomes is paralleled by an increase in the frequency of double-strand breaks (DSBs) during meiotic prophase I, since these are required for HR. We thus investigated the presence, in B-carrying and B-lacking individuals, of the Ser-139 phosphorylated form of the H2AX histone (γH2AX), a modification that occurs in the vicinity of DSBs and thus serves as signal for the DNA-repair events (Zhou and Elledge 2000; Cabrero et al. 2007a). Although we did not observe qualitative differences for γH2AX between +B and –B individuals at prophase I cells, we noticed the presence of conspicuous *foci* of this protein at centromeric regions of all chromosomes during metaphase I. This hinted at the interesting possibility that centromeres might be experiencing frequent DSBs during chromosome segregation. To answer this question, we engaged in the current work in which we analyze the location of several proteins involved in the two main pathways of DNA DSB repair. i.e. Rad51 (involved in the HR pathway) and Ku70 and Ku80 (involved in the NHEJ pathway). We especially focused on any possible location of these proteins at the centromeric region and whether, in addition to their DNA DSB repair role, such centromeric location means an involvement of these proteins in the centromeric function. We initially based our work on immunofluorescence microscopy and, in order to verify the immunofluorescence results, we carried out RNAi-mediated knockdown of the Ku70 gene in *E. plorans*.

In this paper we show that, in the grasshopper *E. plorans*, Rad51 and Ku80 are not found in centromeric regions, but Ku70 is conspicuously present at centromeres during diakinesis, metaphase I, anaphase I, metaphase II and anaphase II, as well as at

spermatogonial and embryonic mitotic metaphases. However, these large centromeric *foci* of Ku70 failed to appear after RNAi-mediated knockdown of the *Ku70* gene, and also after colchicine treatment, suggesting a microtubule-dependent centromere-related function of Ku70. Unexpectedly, the centromeric location of Ku70 seems to be exclusive to *E. plorans*, since 14 other grasshopper and locust species, as well as the domestic mouse, failed to show it.

Materials and methods

Materials

Adult males of the grasshopper *Eyprepocnemis plorans* were collected at a B-carrying population (Torrox, Málaga, Spain), and two B-lacking populations (Socovos and El Gallego, Albacete, Spain). Developing embryos of *E. plorans* were obtained by incubating eggs laid by gravid females bred in the laboratory. We also analyzed the grasshopper species *Heteracris adspersa* (Agramon, Albacete, Spain) and *H. litoralis* (Torrox, Málaga, Spain), which are close relatives of *E. plorans* also belonging to the subfamily Eyprepocneminae. In addition, we analyzed other distantly related grasshopper and locust species collected in the Granada province (Spain), including *Aiolopus strepens*, *Locusta migratoria*, *Oedipoda coerulescens*, *Sphingonotus azurescens* and *Acrotylus insubricus* (subfamily Oedipodinae), *Calliptamus barbarus* (subfamily Calliptaminae), *Dociostaurus jagoi*, *D. maroccanus*, *Chorthippus vagans*, *Ch. jacobsi*, *Omocestus panteli* (subfamily Gomphocerinae) and *Schistocerca gregaria* (subfamily Cyrtacanthacridinae) (this latter from our laboratory colony). Furthermore, we analyzed the domestic mouse. No specific permits were required for the field

studies. The locations sampled were not privately owned or protected in any way, and this study did not involve endangered or protected species.

Slide preparations and inmunofluorescence

Fixation and squash preparations of grasshopper testis follicles and embryos as well as the mouse seminiferous tubules, were performed as described in Cabrero et al. (2007a). In brief, all materials were fixed in freshly prepared 2% paraformaldehyde in PBS (phosphate-buffered saline) containing 0.05% Tween 20 for 15 min. Testis preparations were made by squashing two testis tubules in a small drop of the paraformaldehyde fixative. After immersion into liquid nitrogen and coverslip removal, the slides were immediately transferred into PBS. Cytological preparations of mouse spermatocytes were made following the protocol for grasshopper embryos described in Camacho et al. (1991). Immunofluorescence analysis of γH2AX, Rad51, Ku70, Ku80 and α-tubulin was performed following the methods described in Cabrero et al. (2007a,b). For γH2AX immunofluorescence, we used a monoclonal mouse antibody (Upstate) raised against amino acids 134-142 of the human histone H2AX (Cabrero et al. 2007a; Paull et al. 2000). For Ku70 we used H-308 (Santa Cruz Biotechnology Inc., CA, USA), a rabbit antibody raised against aminoacids 302-609 of the human Ku70. For Ku80, we used sc-1485 (Santa Cruz Biotechnology Inc., CA, USA) a goat antibody raised against a peptide mapping at the C-terminus of the Ku80 of mouse origin. For Rad51 we employed R-1528 (Sigma), a rabbit antibody raised against aminoacids 24-41 of the human Rad51. For α-tubulin, we used (B-5-1-2):sc-23948 (Santa Cruz Biotechnology Inc., CA, USA), a mouse monoclonal antibody raised against sperm axonemes of the sea urchin *Strongylocentrotus purpuratus*. Preparations were washed in PBT, mounted in DAPI-

Vectashield mounting medium, and observed in an epifluorescence microscope. The images were recorded with a cooled CCD camera and optimized for contrast and brightness with The Gimp freeware. In all cases, a negative control was performed by adding PBT instead of the primary antibody. Images were acquired in an Olympus BX41 fluorescence microscope with a DP70 camera, and were optimized for levels, brightness and contrast with The Gimp freeware.

RNAi knockdown

To verify the Ku70 immunostaining results and discard false positives, three males were injected with 5µg of a double stranded RNA corresponding to the *E. plorans Ku70* gene region coding for the same amino acids (302-609) used for generating the H-308 antibody. Using our local blast library of all the arthropodan sequences found in the public databases we identified the *Ku70* regions that are conserved among arthropoda. Two pairs of primers were then used for two nested-design PCR reactions, being GGAGTCATACAATGCGGGCCTA and CTCAGCCATAGCATCCACGTC the forward and reverse primers for the outer PCR and CAAAGGCATATGATGGATTTCA and GAAATTTAGTGCCATAGCTTCCA the forward and reverse primers for the inner PCR. As template, the outer PCR used *E. plorans* cDNA, whilst the inner PCR used the amplicons yielded by the outer primers. Both reactions were performed for 35 cycles at 55ºC annealing temperature and 30 s extension time. DNA from the inner PCR reaction was cleaned, using the Qiagen PCR Clean Kit, sequenced for confirmation (GenBank Accession Number: JX979131), and transcribed from both ends using the standard Ambion T7 RNA polymerase transcription protocol. To ensure knockdown and significant decrease in protein levels,

animals were subjected to two injections with the double stranded RNA. The second injection was carried out 8 days after the first one and, to ensure efficient delivery of the double stranded RNA, both were made intra-abdominally at testis level. One male was sacrificed and immunostaining was carried out on its testis follicles 18 days from the first injection (dffi). Twelve days later (i.e., 30 dffi), two other males were vivisected to extract a few testis follicles for immunostaining without sacrificing the animals. These were not sacrificed until the 53rd dffi. This way we obtained two temporally consecutive samples for immunostaining from the same RNAi individuals.

Quantitative PCR

To test the efficiency of the RNAi knockdown, we analyzed the expression level of the *Ku70* gene by means of quantitative PCR (qPCR) in three males which total RNA was extracted, using the REAL Total RNA spin plus kit (Durviz S.L.U.), at 8, 18 and 53 dffi. Genomic DNA was removed by DNAse I treatment (REAL Star kit —(Durviz S.L.U.), and the quantity and quality of the total RNA was determined using Tecan's Infinite 200 NanoQuant as well as by gel electrophoresis. 100 ηg of total RNA were reverse transcribed using the oligo(dT) primer and SuperScript III First-Strand Synthesis SuperMix kit (Invitrogen). For each analysis, a negative control devoid of reverse transcriptase was included to test for contaminating DNA. PCR amplification of a glyceraldehyde-3-phosphate dehydrogenase (GAPDH) sequence was carried out on each cDNA and control as described in Van Hiel et al. (2009). This way we ensured that the cDNA was properly synthesized and free of contaminating DNA. Prior to using it for the qPCR, each cDNA was diluted with sterile, nuclease free, double distilled water to a 1:5 ratio.

QPCR testing was carried out on different samples and for each of the seven candidate genes suggested for qPCR normalization by Van Hiel et al. (2009). Of these, two genes, namely glyceraldehyde-3-phosphate dehydrogenase (GAPDH) and ribosomal protein 49 (RP49), were highlighted by the geNorm algorithm (Vandesompele et al. 2002) as the most stably expressed. Consequently, we used them as reference genes for our qPCRs. Primers for the qPCR on the target gene (Ku70-F: CACGTCTGGCATTGTTGA, Ku70-R: TCCAGAAGATGCGACAGC) was designed by using the Primer3 web utility (Rozen and Skaletsky 2000), and for the reference genes, we used the primers GADPH-F: GTCTGATGACAACAGTGCAT, GADPH-R: GTCCATCACGCCACAACTTTC, RP49-F: CGCTACAAGAAGCTTAAGAGGTCAT, and RP49-R: CCTACGGCGCACTCTGTTG, as in Vandesompele et al. (2002). QPCR was conducted using the Chromo 4 System CFB-3240 (BIO-RAD) and Sensimix SYBR kit (BIOLINE). Each reaction was run in duplicate and contained 5µl of Sensimix, 5µl of cDNA template (equivalent to 5ng of total RNA) along with 1µl (10pmol) of each primer and 3µl of ddH_20. Cycling parameters were 95ºC for 10 min, then 40 cycles of 94ºC for 15s, 56ºC for 15s and 72ºC for 15s, with a plate-read after each extension (*i.e.*, 72ºC) step. To verify that only a single product was amplified in every reaction, melting curves were performed between each 72ºC and 95ºC step, with a plate-read every 1ºC. A standard curve was used to estimate the efficiency of each primer pair as 2.00 for Ku70, 1.97 for GADPH and 1.99 for RP49. Ku70 expression levels were calculated according to the Pfaffl's method (Pfaffl 2001) and normalized as described in Vandesompele et al. (2002).

Colchicine treatment

To analyze a possible relationship of Ku70 with centromeric function, two additional *E. plorans* males were used for testing the effect of cochicine treatment on the immunostaining results. One was injected with 0.3 ml of 0.1% colchicine in insect saline solution 6 h prior to immunofluorescence analysis while the other was vivisected to extract few testis follicles prior to similar colchicine injection. This enabled an analysis of meiotic cells from the same male both with (after) and without (before) the colchicine treatment.

DNA content in macrospermatids

The amount of DNA in normal and macrospermatids was measured using the Feulgen Image Analysis (FIA) technique described in Ruiz-Ruano et al. (2011).

Results

Ku70 is located at the centromeres of *E. plorans* chromosomes

Immunofluorescence analysis showed centromeric colocalization of Ku70 and γH2AX at meiotic metaphase I (Figure 1). During most first meiotic prophase, however, Ku70 was scarce (Fig. 2a-h), in accordance with previous results in yeast (Åström et al. 1999; Lee et al. 1999) and mouse (Goedecke et al. 1999). The centromeric location of Ku70 was first seen at diakinesis (Fig. 2i-j), and remained apparent through metaphase and anaphase stages during both meiotic divisions (Fig. 2k-p). The centromeric location of these *foci* is inferred from the fact that all chromosomes are telocentric (rod-shaped) and

the presence, in anaphase II cells, of Ku70 signal only in the pulling ends of the segregating chromosomes (see Fig. 2p). The transient presence of Ku70 at centromeric regions, at stages where the nuclear envelope has already been broken down, suggests that this protein might be located on the kinetochore. Immunofluorescence analysis also showed the absence of centromeric *foci* for Ku80 at metaphase I cells (Fig. 2q-r). Although we observed abundance of Rad51 during early first prophase stages, in agreement with the involvement of this protein in HR (Viera et al. 2004; Calvente et al. 2005), no trace of this protein was observed at metaphase I (Fig. 2s-t).

The centromeric location of Ku70 in *E. plorans* is associated with centromere function

The presence of one centromeric Ku70-*focus* per "segregating unit" is remarkable. In fact, we observe one centromeric Ku70-*focus* per homologous chromosome at metaphase I and one per sister chromatid at metaphase II. This coincides with the fact that centromeres separate two homologous chromosomes at metaphase I and two sister chromatids at metaphase II, thus suggesting the functional presence of Ku70 at the centromere.

Colchicine effect on Ku70 immunofluorescence pattern was analyzed in two *E. plorans* males, one of them tested both before and after colchicine injection. With no colchicine, the results were similar to those in non-injected males, with large Ku70 *foci* located on all centromeres (Fig. 3a-b). In both males, the centromeric *foci* of Ku70 disappeared after colchicine injection (Fig. 3c-d). Since colchicine impedes microtubule formation (for review, see Rieder and Palazzo 1992), this result suggests that the presence of Ku70 in the centromere depends on the presence of microtubules. An association between the presence of Ku70 on the centromeres and the latter´s

microtubule-dependent function can therefore be established.

RNAi knockdown of the *Ku70* gene abolishes the centromeric *foci* of Ku70

Since the antibody employed (H-308, from Santa Cruz Biotechnology) is a rabbit polyclonal antibody raised against human Ku70, and to rule out the possibility that our immunofluorescence results might be false positives caused by potential H-308 cross-reactivity with an epitope from a centromeric protein instead of Ku70, we designed two primer pairs for a nested PCR amplification of the region of the *E. plorans Ku70* gene homologous to the 302-609 amino acids region of the human Ku70, and we synthesized double stranded RNA for RNA interference and *Ku70* gene knockdown in *E. plorans*. Quantitative PCR analysis showed that the expression of the *Ku70* gene was very low in RNAi males analyzed at 8 or 18 days from first injection (dffi) and it was considerably higher in the male analyzed at 53 dffi (Fig. 3e), suggesting that males whose Ku70 gene was knocked-down were not only viable, likewise Ku-deficient mice males (Nussenzweig et al. 1996; Gu et al. 1997), but also that they were able to recover this gene expression —as expected given the transient nature of the RNAi-mediated gene knockdown technique.

In contrast to control males (Fig. 3f-g), none of the examined cells from the testis of the three RNAi males showed immunostaining signal for Ku70 on the centromeres (Fig. 3h-i), indicating that the large *foci* observed in normal cells actually correspond to genuine detection of the Ku70 protein on the centromeres. Still, the RNAi males showed some immunostaining signals, indicating the presence of Ku70 in the cytosol and also in the spermatids, as previously shown for normal spermatids in this species (Cabrero et al. 2007b). The detectable signals in the cytosol of the RNAi cells

are due to the knockdown, not silencing, effect of the RNAi technique, whereas the spermatid signals highlight the refractory nature of the mature germ-line cells to RNAi (Singson 2001). Remarkably, we did not find anaphase cells in any of the three RNAi males shown in Table 1, even after analyzing their complete set of testis tubules.

Ku70 knockdown males show polyploid spermatids

To look for possible adverse effects resulting from potential impairment of the correct functioning of the centromere after inactivation of the *Ku70* gene, we analyzed 811-1715 spermatids from each of the three RNAi males and the control males employed for our experiments (Table 1). All RNAi males showed the presence of macrospermatids of several sizes (Fig. 4). Estimations of the DNA amount, by means of the Feulgen Image Analysis (FIA) technique, indicated the presence of 2C, 4C, 8C and 16C spermatids. In addition, microspermatids were also observed, although at much lower frequency than macrospermatids (Table 1).

The quantitative analysis of the frequency of macrospermatids, shown in Table 1, indicated the existence of a basal proportion of macrospermatids in control males (0.21-1.16%). In RNAi males, however, we found a significant increase in this proportion which varied with time since RNAi injection: it increased 2.27-fold in the male analyzed at 18 dffi, 75.87-fold and 87-fold in the two males analyzed at 30 dffi, and 11.86-fold and 3.07-fold in these same males analyzed at 53 dffi. This suggests that the effects of *Ku70* knockdown on macrospermatid formation are not observed until one meiotic cycle has been completed. The basal frequency of microspermatids in the control males was very low (0.12-0.31%), and its frequency was about similar in the 18 dffi male (0.15%), 3.7% and 1.3% in the two 30 dffi males, and 0.18% and 2.8% in

these same males analyzed at 53 dffi. Therefore, the most conspicuously observable change associated with RNAi treatment was an increase in the frequency of polyploid spermatids.

Centromeric Ku70 *foci* are also present during mitosis

To analyze whether the centromeric location of the Ku70 protein is exclusive to meiosis or it also occurs during mitosis, we analyzed mitotic metaphases in spermatogonia from adult males as well as in two types of embryonic cells. In addition to the small *foci* scattered throughout the cytosol, large *foci* of Ku70 were present on the centromeric regions of the chromosomes of all three types of cells analyzed (Fig. 5a-d; Fig. S1). We therefore conclude that Ku70 is associated with centromeric function in both meiotic and mitotic cells.

The centromeric *foci* of Ku70 are dependent on tubulin presence

To ascertain whether Ku70 presence at centromere regions during metaphase and anaphase is dependent on the presence of microtubules, we performed double immunofluorescence analysis with antibodies against Ku70 and α-tubulin on colchicine and control males. As Fig. 5 shows, in the absence of colchicine, mitotic anaphase cells show conspicuous *foci* of Ku70 on the chromosome ends that locate close to the cell poles, in close association with α-tubulin (Fig. 5a-d). Likewise, meiotic metaphase I cells showed abundant α-tubulin across the cytosol, rounding all bivalents, and Ku70 centromeric *foci* were adjacent to α-tubulin (Fig. 5e-h). However, in males injected with colchicine, α-tubulin was very scarce or absent in the most part of the cytosol, and Ku70

centromeric *foci* were absent, with the remarkable few exceptions in those bivalents that were placed at the periphery of the cell where the amount of α-tubulin was higher (Fig. 5i-l).

The novel centromeric function of Ku70 appears to be an autapomorphy in *E. plorans*

To test whether the newly discovered centromeric function of Ku70 is a general characteristic that also occurs in other species, we analyzed the Ku70 immunocytochemical pattern in 14 additional grasshopper and locust species (including *Heteracris adspersa* and *H. litoralis,* as close relatives of *E. plorans,* and the swarming locusts *Locusta migratoria* and *Schistocerca gregaria*), as well as the mouse as a vertebrate representative. In all cases, Ku70 was present at metaphase I, forming numerous small *foci* in the cytosol (Fig. S2) but, opposed to what we report for *E. plorans*, no concentration of Ku70 at centromeric regions was observed in any of the other species. This indicates that the centromere-related function of Ku70, which we report here, might be exclusive to *E. plorans*. However, in the 14 other grasshopper and locust species, as in *E. plorans*, Ku70 was abundant in the nucleus of the elongating spermatids as well as in the sperm tail (Cabrero et al. 2007b), suggesting that, aside from the centromeric function, Ku70 seems to fulfill similar functions in *E. plorans* and other grasshopper species.

The centromeric function of Ku70 is not an adaptation to supernumerary chromosomes

Since *E. plorans* shows a very widespread polymorphism for supernumerary (B) chromosomes, the new function we report here for Ku70 might conceivably be a

byproduct of the presence of these supernumerary chromosomes and/or of the arms race between them and the chromosomes of the standard genome. To assess this possibility, we analyzed the immunofluorescence pattern of Ku70 in individuals with and without B chromosomes from a B-carrying population as well as individuals from two non-B-carrying populations. In all cases, we observed large *foci* of Ku70 on the centromeres of all chromosomes, including the B chromosomes, suggesting that the centromeric location and function of Ku70 is a general characteristic for this species, at least in the populations analyzed in this work. Hence the centromeric function of Ku70 does not seem to be an adaptation to the presence of supernumerary chromosomes in *E. plorans*.

Discussion

RNAi efficiently knocks down the Ku70 gene

The first report proving the possibility of RNAi mediated gene knockdown and the presence of the *sid1* gene in an orthopteran species was in *Schistocerca americana* (Dong and Friedrich 2005). Our experiment with another orthopteran species further proves that RNAi is a valid technique for inactivating genes in orthoptera. Indeed, we observed a close correspondence between double stranded RNA administration and a decrease of the *Ku70* gene expression followed by the disappearance of this gene product from centromeres and a subsequent high increase in the frequency of polyploid spermatids. This gene knockdown effect must be due to the presence in orthopteran species of the double stranded RNA uptake membrane protein SID1 as well as the DICER and all the protein components of the RNA-Induced Silencing Complex. Interestingly, RNAi did not inhibit the presence of Ku70 in mature and developing

spermatozoa, with spermatids and spermatozoa of injected males showing the same normal ($Ku70^{+}$) pattern previously shown in (Cabrero et al. 2007b). At first sight, Ku70 presence in sperm from RNAi males might appear to contradict the validity of the gene silencing technique. However, this result is logical if one bears in mind that spermatozoa seem to be refractory to RNAi even in *Caenorrhabditis elegans*, the model species for RNAi experimentation (see Singson 2001).

The Ku70 protein gathers at the centromeric region of the chromosomes in *E. plorans*

We have observed that the Ku70 monomer of the Ku heterodimer is conspicuously present on the centromeres during the mitotic and meiotic stages of active chromosome segregation whereas the Ku80 monomer fails to show this pattern, suggesting that Ku70 might play a Ku80-independent centromeric function in the grasshopper *E. plorans*. The disappearance of the centromeric *foci* of Ku70 after colchicine injection, in parallel with a decrease in α-tubulin amount, suggests that the putative centromeric function of Ku70 might have something to do with microtubule association to kinetochore regions, since colchicine is a microtubule-targeted agent that binds to α and β subunits of tubulin heterodimers to inhibit its polymerization (for review, see Bhattacharyya et al 2008). In fact, the close association between Ku70 and α-tubulin presence in metaphase I cells from males injected with colchicine indicates that the centromeric function of Ku70 is tubulin dependent (see Fig. 5i-l). Bearing this in mind, the disappearance of Ku70 from the centromeric region in all chromosomes of RNAi males, along with the absence of anaphase cells, suggest a general failure in chromosome segregation leading to cytokinesis failure and the appearance of polyploid spermatids. In fact, completion of cytokinesis requires accurate chromosome segregation in human cells since even non-disjunc-

tion for a single chromosome may result in tetraploid instead of aneuploid cells (Shi and King 2005). Remarkably, also in human cells, it has been shown that Ku70 interacts with ARF6, a protein localized in the cleavage furrow and midbody of mitotic cells, and whose activity is regulated during cytokinesis (Schweitzer and D'Souza-Schorey 2005).

The exclusive presence of even ploidy levels in spermatids, and the absence of anaphase cells, indicate the occurrence of cytokinesis failures and restitution processes, an expected result of an impairment of kinetochore-microtubule association leading to cytokinesis failure (Normand and King 2010). Bearing in mind that a primary spermatocyte is 4C, the presence of polyploid spermatids with ploidy levels higher than 4C suggests that these cytokinesis failures can also occur during preceding spermatogonial mitoses (see Fig. S3a). For instance, 2C spermatids would result from failure in the second meiotic division, whereas 4C ones would result from failures in both meiotic divisions, 8C from failures in the last spermatogonial mitosis plus both meiotic divisions, and 16C in the two last spermatogonial mitoses plus both meiotic divisions. The differences in ploidy level of the resulting spermatids thus rest on the timing of double stranded RNA uptake and processing by the different dividing cell types (spermatogonium, primary spermatocyte or secondary spermatocyte) (see some examples in Fig. S3).

As to the dynamics of the above mentioned spermatid malformations, our results show only a slight increase in the frequency of macrospermatids during the first 18 days post-RNAi treatment, then a much steeper rise of the prevalence of these mis-formed spermatids during the following 12 days (*i.e.*, at 30 dffi; see Table 1). This is consistent with the fact that the complete meiotic cycle in grasshoppers lasts about 20 days (Fox et al. 1974), so that at 18 dffi only a few RNAi spermatocytes had completed meiosis and thus were affected by the *Ku70* gene knockdown, whereas, 12 days later, many more cells had had time to finish meiosis and manifest cell division problems.

Ku70 is a transient centromeric passenger presumably involved in microtubule anchoring

The absence of colocalization of Ku80 in the centromeric *foci* of Ku70 indicates that the latter is not there for DNA repair purposes. Likewise, its centromeric presence does not appear to be a consequence of interactions with HP1α, since RNAi knockdown of *HP1α* fails to eliminate the centromeric *foci* of Ku70 (Ruiz-Estévez et al., in preparation). In order to look for other conceivable functions of Ku70 at centromeric level, diverse biological functions can be inferred from its ability to bind other proteins. One of these, clusterin (Yang et al. 1999), is a chaperone-like molecule that interacts with the microtubule-destabilizing protein SCLIP of the stathmin family (Kang et al. 2005). The fact that colchicine prevents the centromeric location of Ku70 (see Fig. 3) suggests that Ku70 may have a thus far unreported microtubule-dependent function at *E. plorans* centromeres. Additional support to this conclusion comes from our observation that Ku70 seems to also have a microtubule-dependent function in the formation of the sperm tail both in *E. plorans* and all the 14 other orthopteran species studied in this work (Cabrero et al. 2007b), so that the Ku70 function at both centromeres and sperm tail could be rather similar.

The presence of polyploid spermatids in Ku70 RNAi-knocked-down males indicates that many spermatocytes finished meiosis despite the absence of Ku70 at centromeres and the presumed problems in microtubule anchoring, thus surpassing the spindle assembly checkpoint (SAC) control. Among the dynamic protein components of the kinetochore, the SAC components reach their maximum concentration in the absence of microtubules (Howell et al. 2004), just the opposite pattern of Ku70 in *E.*

plorans, which is not present 6h after colchicine injection. This indicates that the Ku70 centromeric function reported here is different from the canonical SAC function.

A more suggestive possibility is an interaction with some kinetochore proteins, e.g. the APC (adenomatous polyposis coli) and/or EB1 (end binding 1) proteins, which associate to kinetochores only when microtubules are anchored (Kaplan et al. 2001; Tirnauer et al. 2002) thus resembling the transient presence of Ku70 on the *E. plorans* cenromeres. Remarkably, siRNA-mediated inhibition of APC, EB1, or APC and EB1 together gives rise to spindle defects without mitotic arrest (Green et al. 2005), and APC inhibition produces polyploidy (Dikovskaya et al. 2007), i.e. exactly the same consequences as Ku70 knockdown in *E. plorans*. A possible microtubule anchoring function of Ku70 at the kinetochores of *E. plorans* is thus conceivable through interaction with APC and EB1. This microtubule-dependent function of Ku70 could operate at kinetochores (exclusively in *E. plorans*) but also at the centriolar adjuncts of spermatids in all grasshopper species (Cabrero et al. 2007b).

APC and EB1 belong to a group of proteins showing affinity for the plus-ends of growing microtubules (+TIPs). It is thus conceivable that Ku70 binds the +TIPS and it concentrates in the kinetochore when bundles of microtubules reach it. Indeed, the fact that the spindle microtubules are sensitive to colchicine disruption (Bhattacharyya et al 2008), supports our observation that colchicine treatment in *E. plorans* prevents the presence of Ku70 at centromeres and is consistent with Ku70 involvement in a microtubule-dependent centromeric function. Therefore, the Ku70 function that better explains its transient presence at centromeric regions is probably related to the kinetochore-microtubule anchoring that allows accurate chromosome segregation.

The centromeric function of Ku70 is an autapomorphy

In this work we analyzed a high number of grasshopper and locust species (14 including *E. plorans*, two of its closely related species and the well known pest locusts *Locusta migratoria* and *Schistocerca gregaria*), as well as the mouse. Among these, only *E. plorans* showed centromeric presence of Ku70. Still, we cannot categorically rule out that it might be present in other organisms not yet examined. In fact, in human cells, it has recently been shown that DNA-PKcs, with which Ku70 and Ku80 form the DNA-dependent protein kinase (Gell et al. 1999), is activated and phosphorylated in close association with the spindle apparatus at centrosomes and kinetochores, thus suggesting that, in addition to its role in DSB repair, DNA-PKcs (and perhaps Ku too) is a critical regulator of mitosis and could modulate microtubule dynamics in chromosome segregation (Lee et al. 2011).

Whatever the case, the absence of Ku70 at the chromosome centromeres of 14 orthopteran and 1 vertebrate species strongly suggests that Ku70 binding to the centromere is most likely an autapomorphy in *E. plorans* and that the ancestral Ku70 state did not include a centromeric function. Since most of the functions of Ku are not directly related to each other, establishing the evolutionary history of this protein might be challenging (Tuteja and Tuteja 2000), and the centromeric location of Ku70 during mitotic and meiotic metaphase and anaphase in *E. plorans* is a clear evidence of the complex evolutionary pathways that this protein may have followed in parallel to the acquisition of its multiple functions. Interestingly, Scherthan and Trelles-Sticken (2008) showed that the absence of Ku interferes with the ordered occurrence of chromosome dynamics during first meiotic prophase, and Shuaib et al. (2010) found the presence of both Ku70 and Ku80 among the proteins associated with e-CENP-A in prenucleosomal complexes purified by immunoprecipitation from HeLa cell extracts, suggesting that

Ku70 might perform thus far undiscovered and previously unrecognized centromeric functions not only in the grasshopper *E. plorans* but in other organisms too.

Acknowledgements We thank R. Jiménez for providing us with mouse spermatocytes, M. Ruiz-Estévez for giving us an *E. plorans* cDNA aliquote, and T. López for technical assistance. This study was supported by grants from the Spanish Ministerio de Ciencia e Innovación (CGL2009-11917 and BFU2010-16438) and Plan Andaluz de Investigación (CVI-6649), and was partially performed by FEDER funds. M. Bakkali was supported by a Ramón y Cajal fellowship from the Spanish Ministerio de Ciencia e Innovación.

References

Åström SU, Okamura SM, Rine J (1999) Yeast cell-type regulation of DNA repair. Nature 397: 310

Bhattacharyya B, Pnada D, Gupta S, Banerjee M (2008) Anti-mitotic activity of colchicine and the structural basis for its interaction with tubulin. Medicinal Research Reviews 28: 155-183

Bertinato J, Schild-Poulter C, Hache RJG (2001) Nuclear localization of Ku antigen is promoted independently by basic motifs in the Ku70 and Ku80 subunits. J Cell Sci 114: 89–99

Cabrero J, Teruel M, Carmona FD, Camacho JPM (2007a) Histone H2AX phosphorylation is associated with most meiotic events in grasshopper. Cytogenet Genome Res 116: 311–315

Cabrero J, Palomino-Morales RJ, Camacho JPM (2007b) The DNA-repair Ku70 protein is located in the nucleus and tail of elongating spermatids in grasshoppers.

Chromosome Res 15: 1093–1100

Calvente A, Viera A, Page J et al. (2005) DNA-double strand breaks and homology search: inferences from a species with incomplete pairing and synapsis. J Cell Sci 118: 2957–2963

Camacho JPM, Carballo AR, Cabrero J (1980) The B-chromosome system of the grasshopper *Eyprepocnemis plorans* subsp. *plorans* (Charpentier). Chromosoma 80: 163–176

Camacho JPM, Cabrero J, Viseras E, López-León MD, Navas-Castillo J, Alché JD (1991) G-banding in two species of grasshoppers and its relationship to C, N and fluorescence banding techniques. Genome 34: 638–643

Camacho JPM, Bakkali M, Corral JM et al. (2002) Host recombination is dependent on the degree of parasitism. Proc R Soc B 269: 2173–2177

Dikovskaya D, Schiffmann D, Newton IP et al. (2007) Loss of APC induces polyploidy as a result of a combination of defects in mitosis and apoptosis. J Cell Biol 176: 183–195

Dong Y, Friedrich M (2005) Nymphal RNAi: systemic RNAi mediated gene knockdown in juvenile grasshopper. BMC Biotechnol 5: 25

Fox DP, Hewitt GM, Hall DJ (1974) DNA replication and RNA transcription of euchromatic and heterochromatic chromosome regions during grasshopper meiosis. Chromosoma 45: 43–62

Gao YJ, Chaudhuri J, Zhu CM, Davidson L, Weaver DT, Alt FW (1998) A targeted DNA-PKcs-null mutation reveals DNA-PK-independent functions for KU in V(D)J recombination. Immunity 9: 367–376

Gell D, Jackson SP (1999) Mapping of protein-protein interactions within the DNA-dependent protein kinase complex. Nucl Acids Res 27: 3494–3502

Goedecke W, Eijpe M, Offenberg HH, van Aalderen M, Heyting C (1999) Mre11 and Ku70 interact in somatic cells, but are differentially expressed in early meiosis. Nat Genet 23: 194–198

Green RA, Wollman R, Kaplan KB (2005) APC and EB1 function together in mitosis to regulate spindle dynamics and chromosome alignment. Mol Biol Cell 16: 4609–4622

Gu YS, Seidl KJ, Rathbun GA et al. (1997) Growth retardation and leaky SCID phenotype of Ku70-deficient mice. Immunity 7: 653–665

Gu YS, Sekiguchi J, Gao YJ et al. (2000) Defective embryonic neurogenesis in Ku-deficient but not DNA-dependent protein kinase catalytic subunit-deficient mice. Proc Natl Acad Sci USA 97: 2668–2673

Howell BJ, Moree B, Farrar EM, Stewart S, Fang G, Salmon ED (2004) Spindle checkpoint protein dynamics at kinetochores in living cells. Curr Biol 14: 953–964

Kang SW, Shin YJ, Shim YJ, Jeong SY, Park IS, Min BH (2005) Clusterin interacts with SCLIP (SCG10-like protein) and promotes neurite outgrowth of PC12 cells. Exp Cell Res 309: 305–315

Kaplan KB, Burds AA, Swedlow JR, Bekir SS, Sorger PK, Näthke IS (2001) A role for the Adenomatous Polyposis Coli protein in chromosome segregation. Nat Cell Biol 3: 429–432

Katz DJ, Beer MA, Levorse JM, Tilghman SM (2005) Functional characterization of a novel Ku70/80 pause site at the H19/Igf2 imprinting control region. Mol Cell Biol 25: 3855–3863

Koike M (2002) Dimerization, translocation and localization of Ku70 and Ku80 proteins. J Rad Res 43: 223–236

Koike M, Awaji T, Kataoka M et al. (1999) Differential subcellular localization of DNA-dependent protein kinase components Ku and DNA-PKcs during mitosis. J Cell Sci 112: 4031–4039

Koike M, Shiomi T, Koike A (2001) Dimerization and nuclear localization of Ku proteins. J Biol Chem 276: 11167–11173

Koike M, Koike A (2005) The Ku70-binding site of Ku80 is required for the stabilization of Ku70 in the cytoplasm, for the nuclear translocation of Ku80, and for Ku80-dependent DNA repair. Exp Cell Res 305: 266–276

Lee K-J, Lin Y-F, Chou H-Y et al. (2011) Involvement of DNA-dependent protein kinase in normal cell cycle progression through mitosis. J Biol Chem 286: 12796–12802

Lee SE, Pâques F, Sylvan J, Haber JE (1999) Role of yeast SIR genes and mating type in directing DNA double-strand breaks to homologous and non-homologous repair paths. Curr Biol 9: 767–770

Martinez JJ, Seveau S, Veiga E, Matsuyama S, Cossart P (2005) Ku70, a component of DNA-dependent protein kinase, is a mammalian receptor for *Rickettsia conorii*. Cell 123: 1013–1023

Monferran S, Muller C, Mourey L, Frit P, Salles B (2004a) The membrane-associated form of the DNA repair protein Ku is involved in cell adhesion to fibronectin. J Mol Biol 337: 503–511

Monferran S, Paupert J, Dauvillier S, Salles B, Muller C (2004b) The membrane form of the DNA repair protein Ku interacts at the cell surface with metalloproteinase 9. Embo J 23: 3758–3768

Muñoz E, Perfectti F, Martín-Alganza A, Camacho JPM (1998) Parallel effects of a B chromosome and a mite that decrease female fitness in the grasshopper

Eyprepocnemis plorans. Proc Roy Soc B 265: 1903–1909

Normand G, King RW (2010) Understanding cytokinesis failure. In: Polyploidization and Cancer, edited by Randy Y.C. Poon. Landes Bioscience and Springer Science+Business Media.

Nussenzweig A, Chen C, da Costa Soares V, Sanchez M, Sokol K, Nussenzweig MC, Li GC (1996) Requirement for Ku80 in growth and immunoglobulin V(D)J recombination. Nature 382: 551–555

Paull TT, Rogakou EP, Yamazaki V, Kirchgessner CU, Gellert M, Bonner WM (2000) A critical role for histone H2AX in sequential recruitment of repair factors to nuclear foci after DNA damage. Curr Biol 10: 886–895

Pfaffl MW (2001) A new mathematical model for relative quantification in real-time RT–PCR. Nucl Acids Res 29: 2002–2007

Pöggeler S, Kuck U (2006) Highly efficient generation of signal transduction knockout mutants using a fungal strain deficient in the mammalian ku70 ortholog. Gene 378: 1–10

Rieder CL, Palazzo RE (1992) Colcemid and the mitotic cycle. J Cell Sci 102: 387–392

Rodgers W, Jordan SJ, Capra JD (2002) Transient association of Ku with nuclear substrates characterized using fluorescence photobleaching. J Immunol 168: 2348–2355

Rozen S, Skaletsky HJ (2000) Primer3 on the WWW for general users and for biologist programmers. In: Krawetz S and Misener S (ed) Bioinformatics Methods and Protocols: Methods in Molecular Biology. Totowa, NJ: Humana Press. pp 365–386

Ruiz-Ruano FJ, Ruiz-Estévez M, Rodríguez-Pérez J, López-Pino JL, Cabrero J, Camacho JPM (2011) DNA amount of X and B chromosomes in the

grasshoppers *Eyprepocnemis plorans* and *Locusta migratoria*. Cytogenet Genome Res 134: 120–126

Sawada M, Sun WY, Hayes P, Leskov K, Boothman DA, Matsuyama S (2003) Ku70 suppresses the apoptotic translocation of Bax to mitochondria. Nat Cell Biol 5: 320–329

Scherthan H, Trelles-Sticken E (2008) Absence of yKu/Hdf1 but not myosin-like proteins alters chromosome dynamics during prophase I in yeast. Differentiation 76: 91–98

Schweitzer JK, D'Souza-Schorey C (2005) A requirement for ARF6 during the completion of cytokinesis. Exp Cell Res 311:74–83

Shi Q, King RW (2005) Chromosome nondisjunction yields tetraploid rather than aneuploid cells in human cell lines. Nature 437:1038-1042

Shuaib M, Ouararhni K, Dimitrov S, Hamiche A (2010) HJURP binds CENP-A via a highly conserved N-terminal domain and mediates its deposition at centromeres. Proc Natl Acad Sci USA 107: 1349–1354

Singson A (2001). Every sperm is sacred: fertilization in *Caenorhabditis elegans*. Dev Biol 230: 101–109

Song KY, Jung YS, Jung DH, Lee I (2001) Human Ku70 interacts with heterochromatin protein 1 alpha. J Biol Chem 276: 8321–8327

Takata M, Sasaki MS, Sonoda E et al. (1998) Homologous recombination and non-homologous end-joining pathways of DNA double-strand break repair have overlapping roles in the maintenance of chromosomal integrity in vertebrate cells. Embo J 17: 5497–5508

Tirnauer JS, Canman JC, Salmon ED, Mitchison TJ (2002) EB1 targets to kinetochores with attached, polymerizing microtubules. Mol Biol Cell 13: 4308–4316

Tuteja R, Tuteja N (2000) Ku autoantigen: A multifunctional DNA-binding protein. Crit Rev Biochem Mol Biol 35: 1–33

Vandesompele J, De Preter K, Pattyn F et al. (2002) Accurate normalization of real-time quantitative RT-PCR data by geometric averaging of multiple internal control genes. Genome Biol 3: 7

Van Hiel MB, Van Wielendaele P, Temmerman L et al. (2009). Identification and validation of housekeeping genes in brains of the desert locust *Schistocerca gregaria* under different developmental conditions. BMC Mol Biol 10**:** 56

Viera A, Santos JL, Page J et al. (2004). DNA double-strand-break, recombination and synapsis, the timing of meiosis differs in grasshoppers and flies. EMBO Rep. 5: 385–391

Yang CR, Yeh SY, Leskov K et al. (1999) Isolation of Ku70-binding proteins (KUBs). Nucl Acids Res 27: 2165–2174

Zhou B, Elledge SJ (2000) The DNA damage response: putting checkpoints in perspective. Nature 408: 433–439

Zurita S, Cabrero J, López-León MD, Camacho JPM (1998) Polymorphism regeneration for a neutralized selfish B chromosome. Evolution 52: 274–277

Figure legends

Fig. 1 Colocalization of Ku70 with γH2AX in *E. plorans*. Metaphase I cell showing centromeric immunofluorescence patterns for Ku70 (a), γH2AX (b), a merge of the patterns for both antibodies without (c) and with DAPI staining (d). Bar= 10μm.

Fig. 2 Centromeric location of Ku70 in *E. plorans* spermatocytes. Cells at several meiotic stages are depicted twice, one (on the left) after immunofluorescence with a Ku70 antibody (red) and other (on the right) also including DAPI staining to show chromatin. Note the presence in (i-p) of one large centromeric Ku70 *focus* per segregating unit, i.e. one per homologous chromosome in diakinesis (i,j) and metaphase I (k,l) cells, and one per sister chromatid in metaphase II cells (m,n), with the *foci* of sister chromatids oriented towards opposite poles in anaphase II cells (o,p). The centromeric *foci* of Ku70 (shown in i-p) were observed in 100% of the cells analyzed from 30 untreated males from three different populations. Also note the absence of centromeric *foci* for both Ku80 (q,r) and RAD51 (s,t) in metaphase I cells. Bar= 10μm. B in (l) points the B chromosome.

Fig. 3 Disappearance of the centromeric Ku70-*foci* by both colchicine injection and *Ku70* gene knockdown in *E. plorans* males. Metaphase I cells from control and experimental males from the colchicine (a-d) and RNAi (f-i) experiments. Note the presence of centromeric Ku70-*foci* before colchicine injection (a,b) and their absence after it (c,d). This pattern was observed in 100% of the cells analyzed from the two males analyzed. (e) Quantitative PCR analysis of the expression level of the *Ku70* gene in RNAi males after 8, 18 and 53 days from first injection (dffi). Observe the sharp decrease in expression level (RQ) at 8 and 18 dffi, and the subsequent partial recovery

at 53 dffi. (f,g) Metaphase I cell from a control male (with no RNAi injection), showing presence of large Ku70 *foci* on all centromeres. (h,i) Metaphase I cell after RNAi injection showing absence of centromeric Ku70 *foci*. The patterns shown in (f,g) and (h,i) did not show intraindividual variation either in the two control or the three experimental males analyzed. RQ= Relative Quantification, Bar= 10µm.

Fig. 4 Formation of polyploid spermatids in RNAi males. (a) A microscopic field showing DAPI staining of some normal spermatids (N) along with many macrospermatids (M). (b) DNA content of spermatids, measured by the Feulgen Image Analysis (FIA) technique, and showing to be 1C for normal spermatids, and 2C, 4C, 8C or 16C for macrospermatids (for the number of spermatids analyzed, see Table 1). Bar= 10µm.

Fig. 5 Association of the centromeric *foci* of Ku70 (red) with α-tubulin (green) in a mitotic anaphase (a-d) and meiotic metaphase I (e-h) cells, without colchicine treatment, and in a metaphase I cell (i-l) from a male injected with colchicine. Note the lower amount of α-tubulin in the latter and the presence of several centromeric *foci* of Ku70 in the periphery of this cell in coincidence with higher amounts of α-tubulin (arrows in l). Also note the abundance of Ku70 in spermatid nuclei (arrowhead in h), as previously reported by Cabrero et al. (2007b). Bar= 10µm.

Table 1 Frequency of macro- and microspermatids found in the RNAi and control males. Exp= experiment, Bs= number of B chromosomes, Dffi= days from first injection, N= normal spermatids, M= macrospermatids, m= microspermatids, R_M= ratio of macrospermatids between RNAi and control males, R_m= ratio of microspermatids between RNAi and control males. Contingency chi-squared tests comparing the frequency of macrospermatids between control and experimental males indicated significantly higher proportions in RNAi males: ** indicate P<0.01, *** indicate P<0.001

				Type of spermatids							
Exp	**Type**	**Bs**	**Dffi**	**N**	**M**	**m**	**Total**	**% M**	**R_M**	**% m**	**R_m**
1	Control	1	18	1613	19	5	1637	1.16		0.31	
	RNAi	1	18	1329	36	2	1367	2.63	2.27**	0.15	0.48
2	Control	2	30	1415	3	2	1420	0.21		0.14	
	RNAi_1	3	30	651	130	30	811	16.03	75.87***	3.70	26.26***
	RNAi_2	1	30	1498	323	24	1845	17.51	82.87***	1.30	9.24***
	Control	2	53	1700	13	2	1715	0.76		0.12	
	RNAi_1	3	53	1495	148	3	1646	8.99	11.86***	0.18	1.56
	RNAi_2	1	53	1590	39	47	1676	2.33	3.07***	2.80	24.05***

Supporting Figures

Fig. S1 The centromeric location of Ku70 also occurs during mitosis in *E. plorans*. (a,b) Spermatogonial mitotic metaphase. (c,d) Embryo mitotic metaphase cell. (e,f) Embryo mitotic metaphase from a neuroblast cell (of giant size). Note the presence of centromeric *foci* of Ku70 in the three cells. This was observed in 100% of the analyzed cells. Bar= 10µm.

Fig. S2 Absence of centromeric immunofluorescence signals for Ku70 at meiotic metaphase I in 14 grasshopper species and the mouse. Examples are shown for Ku70 (a,c,e) and DAPI+Ku70 (b,d,f) in the grasshopper species *Omocestus panteli* (a, b) and *Sphingonotus azurescens* (c, d), and the mouse (e,f). Bar= 10µm.

Fig. S3 Presence of polyploid and binucleate cells in RNAi males. a) Two tetraploid spermatogonia at mitotic prometaphase. b) Tetraploid metaphase I cell. c) Binucleate cell.

Figure 1

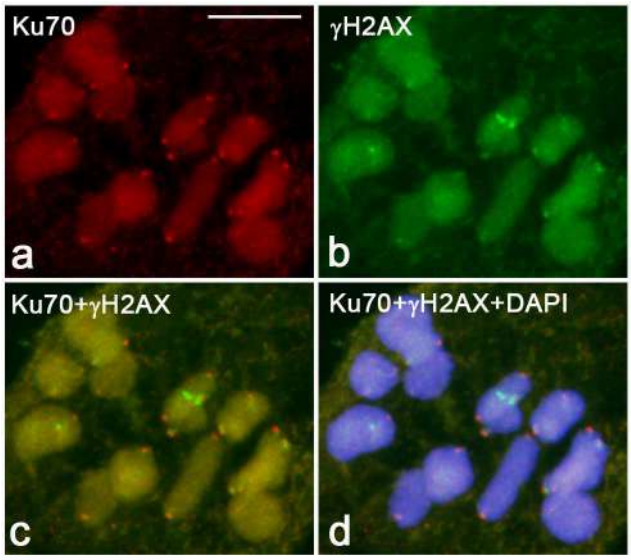

Figure 2

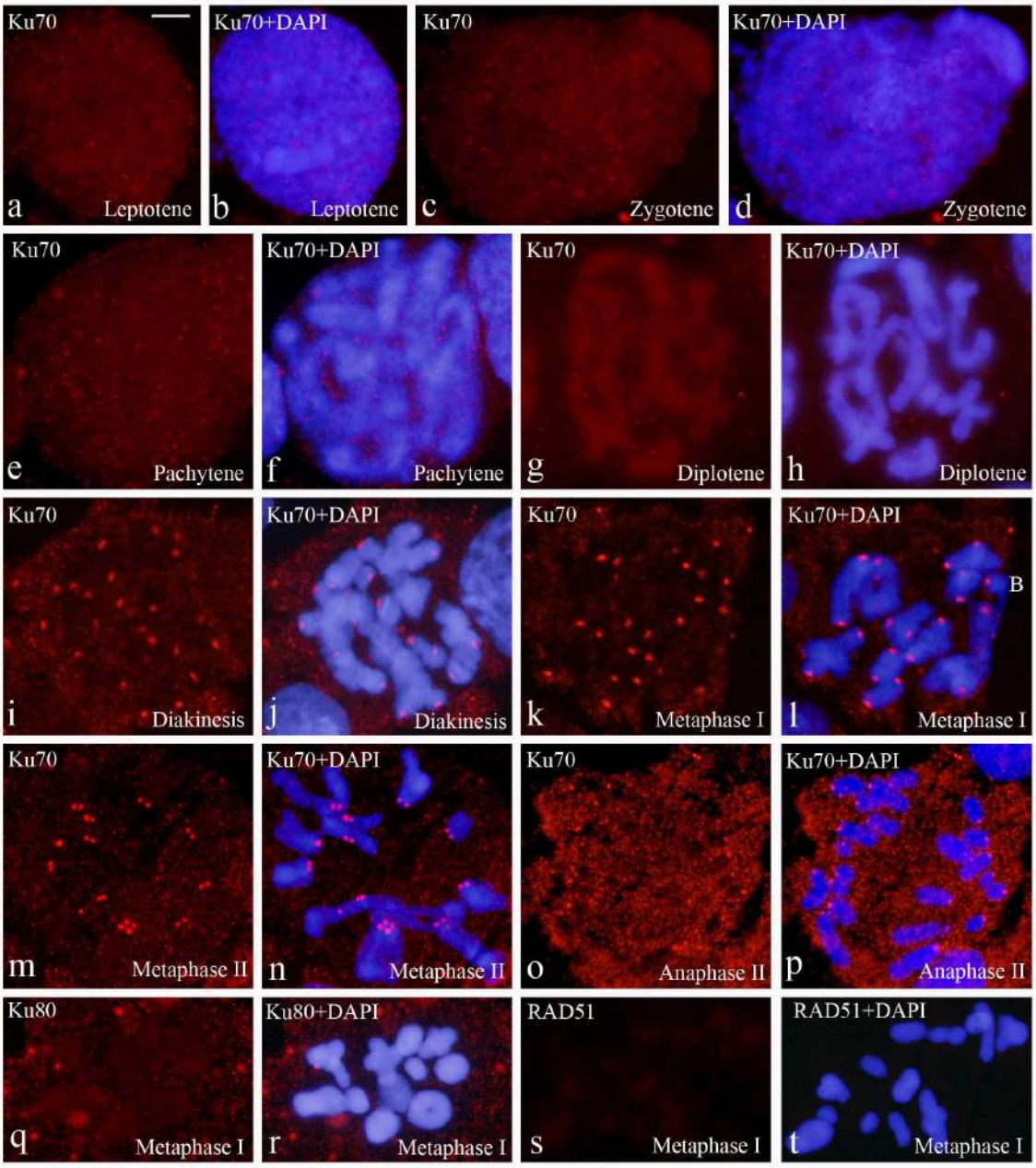
Ku70
a Leptotene
Ku70+DAPI
b Leptotene
Ku70
c Zygotene
Ku70+DAPI
d Zygotene
Ku70
e Pachytene
Ku70+DAPI
f Pachytene
Ku70
g Diplotene
Ku70+DAPI
h Diplotene
Ku70
i Diakinesis
Ku70+DAPI
j Diakinesis
Ku70
k Metaphase I
Ku70+DAPI
B
l Metaphase I
Ku70
m Metaphase II
Ku70+DAPI
n Metaphase II
Ku70
o Anaphase II
Ku70+DAPI
p Anaphase II
Ku80
q Metaphase I
Ku80+DAPI
r Metaphase I
RAD51
s Metaphase I
RAD51+DAPI
t Metaphase I

Figure 3

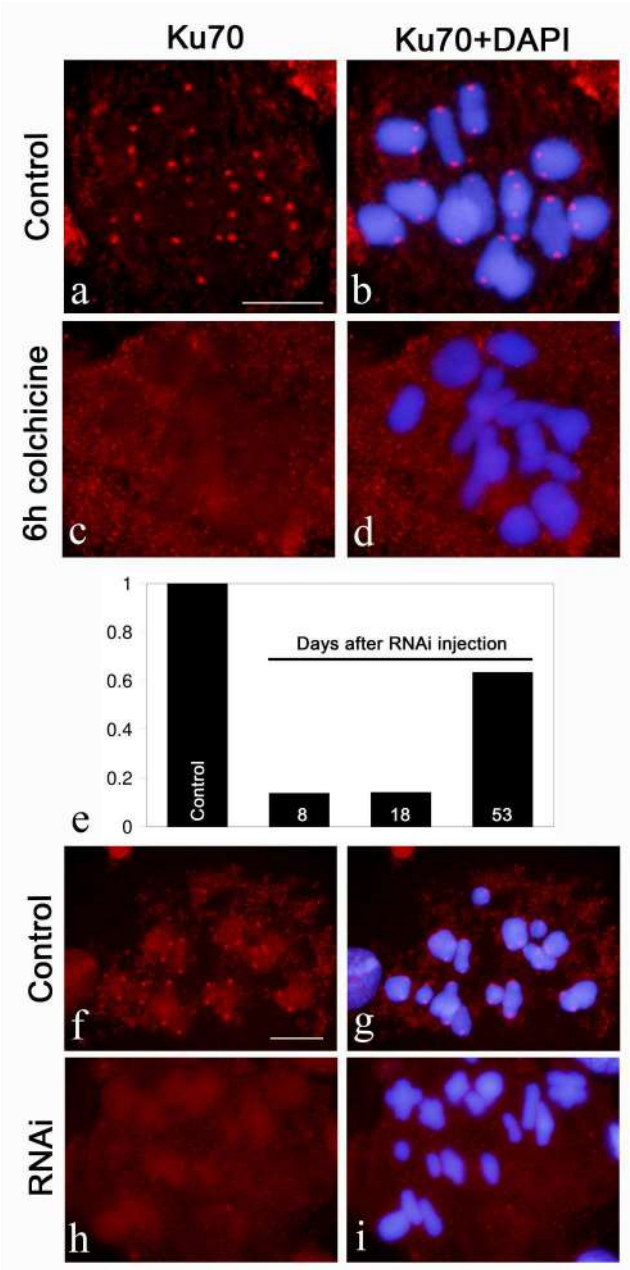
Ku70
Ku70+DAPI
Control
6h colchicine
a
b
c
d
e
1
0.8
0.6
0.4
0.2
0
Control
8
18
53
Days after RNAi injection
Control
RNAi
f
g
h
i

Figure 4

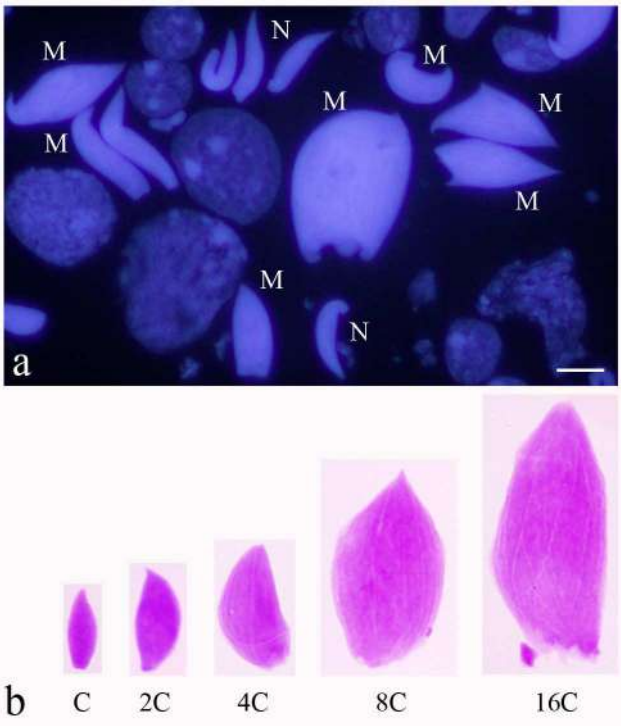

Figure 5

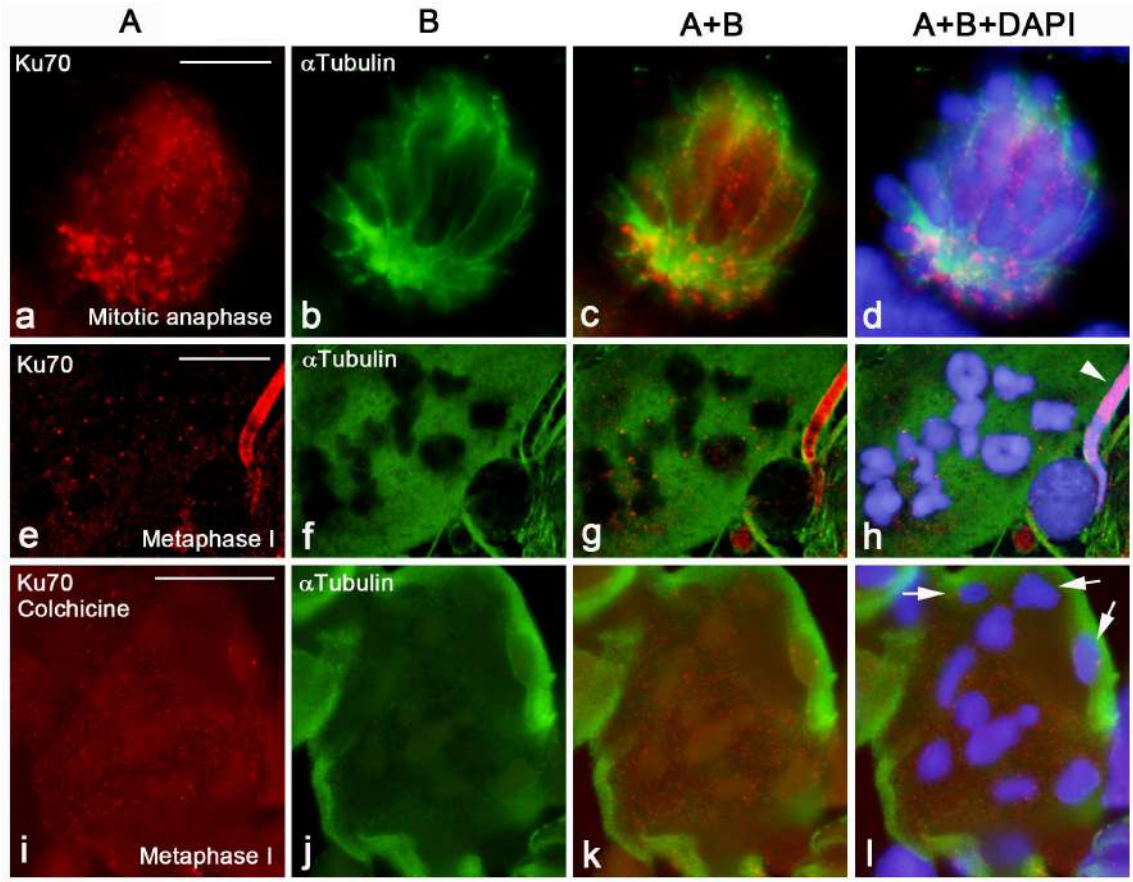
A
B
A+B
A+B+DAPI
Ku70
αTubulin
a
Mitotic anaphase
b
c
d
Ku70
αTubulin
e
Metaphase I
f
g
h
Ku70
Colchicine
αTubulin
i
Metaphase I
j
k
l

Figure S1

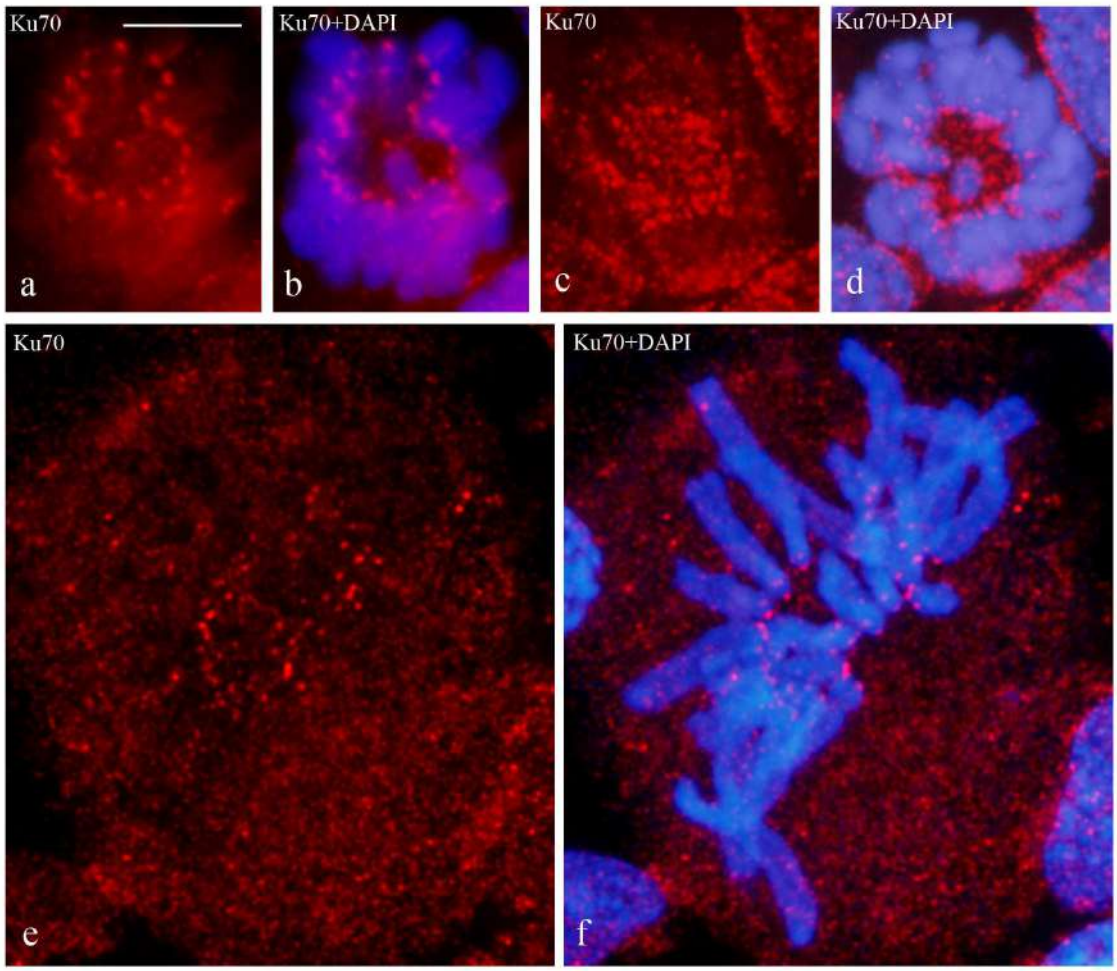

Figure S2

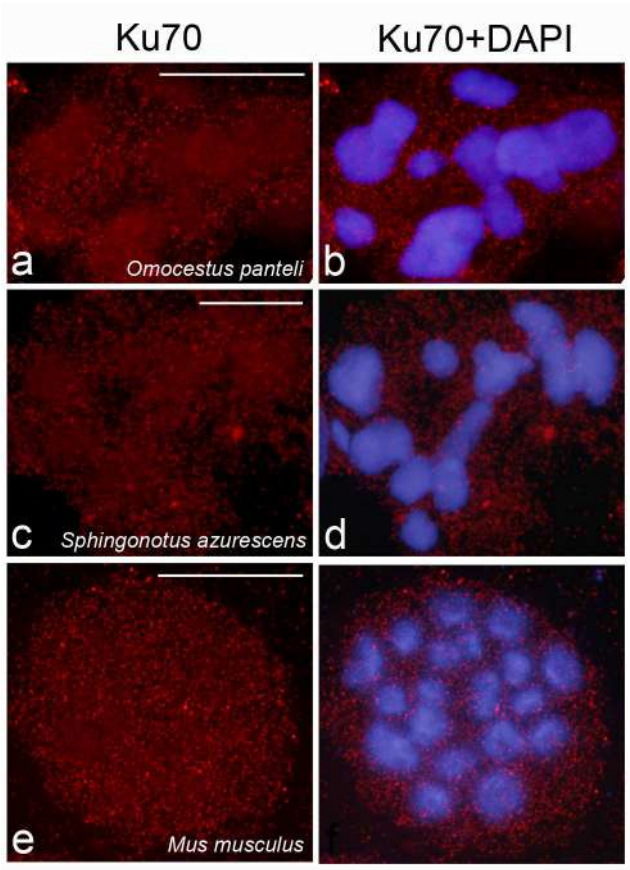
Ku70
Ku70+DAPI
a
Omocestus panteli
b
c
Sphingonotus azurescens
d
e
Mus musculus

Figure S3